

Spin Susceptibility in Non-Centrosymmetric Superconductors with Topological Transition of Fermi Surfaces

Daisuke MARUYAMA^{1*} and Youichi YANASE^{1,2}

¹Graduate School of Science and Technology, Niigata University, Niigata 950-2181, Japan

²Department of Physics, Niigata University, Niigata 950-2181, Japan

The non-centrosymmetric superconductors $\text{Li}_2\text{Pd}_3\text{B}$ and $\text{Li}_2\text{Pt}_3\text{B}$ show different superconducting properties despite having the same crystal symmetry. Motivated by experimental results, we investigate the spin susceptibility of non-centrosymmetric superconductors accompanied by the topological transition of Fermi surfaces due to antisymmetric spin-orbit coupling, which is indicated by the first-principles band structure calculation for $\text{Li}_2\text{Pt}_3\text{B}$. We study three types of topological transition, namely, (A) the disappearance of the Fermi surface, (B) crossing the Dirac point, and (C) crossing the saddle point van-Hove singularity. The spin susceptibility in the superconducting state is increased by the topological transitions (A) and (C), while it is decreased by (B). We discuss the unusual magnetic properties observed in $\text{Li}_2\text{Pt}_3\text{B}$ on the basis of these results.

KEYWORDS: superconductivity without inversion symmetry, topological transition of Fermi surfaces, spin susceptibility

1. Introduction

Recently, superconductors lacking inversion symmetry in the crystal structure have been attracting much attention. The antisymmetric spin-orbit coupling induced by the broken inversion symmetry leads to the spin-splitting of the Fermi surface and gives rise to unique superconducting properties, such as the parity mixing of Cooper pairs.¹⁾

Among many non-centrosymmetric superconductors, the perovskite-like cubic compounds $\text{Li}_2\text{Pd}_3\text{B}$ ²⁾ and $\text{Li}_2\text{Pt}_3\text{B}$ ³⁾ show particularly intriguing properties. The superconducting properties are different between these two compounds in spite of having the same crystal symmetry.^{2–12)} The order parameter is fully gapped in $\text{Li}_2\text{Pd}_3\text{B}$, while it has line nodes in $\text{Li}_2\text{Pt}_3\text{B}$.^{4–7,9,12)} The NMR Knight shift of $\text{Li}_2\text{Pd}_3\text{B}$ is decreased across the superconducting transition temperature T_c , while that of $\text{Li}_2\text{Pt}_3\text{B}$ is mostly unaffected in the superconducting state.^{6,12)} Although these behaviors of $\text{Li}_2\text{Pd}_3\text{B}$ indicate the conventional s-wave superconductivity admixed with the spin triplet p-wave one owing to the antisymmetric spin-orbit coupling, experimental results of $\text{Li}_2\text{Pt}_3\text{B}$ are incompatible with the canonical theory of non-centrosymmetric superconductivity.¹⁾

According to the weak coupling theory neglecting the correlation effects, the spin susceptibility in the cubic non-centrosymmetric superconductor should be reduced to 2/3 of the normal state value at $T = 0$.^{13,14)} On the other hand, the Knight shift measurement of $\text{Li}_2\text{Pt}_3\text{B}$ did not show such a decrease in spin susceptibility.^{6,12)} The spin triplet superconducting state has been proposed for $\text{Li}_2\text{Pt}_3\text{B}$ on the basis of this experimental result,^{6,12)} however, the spin susceptibility at low magnetic fields $\mu_B H \ll k_B T_c$ is independent of the symmetry of the order parameter.¹⁵⁾ Indeed, the pairing states indicated by theoretical studies^{16,17)} are incompatible with the Knight shift measurement of $\text{Li}_2\text{Pt}_3\text{B}$. Although the electron correlation effect may enhance the spin susceptibility in the superconducting state,¹³⁾ such enhancement is unlikely to occur in $\text{Li}_2\text{Pd}_3\text{B}$ and $\text{Li}_2\text{Pt}_3\text{B}$ in which the corre-

lation effect is negligible.^{8,10)} The influence of magnetic order has been pointed out for the heavy fermion superconductor CePt_3Si ;^{18,19)} however, the magnetic order does not occur in $\text{Li}_2\text{Pt}_3\text{B}$. Thus, the superconducting state of $\text{Li}_2\text{Pt}_3\text{B}$ remains controversial, while $\text{Li}_2\text{Pd}_3\text{B}$ is a “conventional” non-centrosymmetric superconductor.

For the difference between $\text{Li}_2\text{Pt}_3\text{B}$ and $\text{Li}_2\text{Pd}_3\text{B}$, a substantial enhancement of antisymmetric spin-orbit coupling has been pointed out for $\text{Li}_2\text{Pt}_3\text{B}$.²⁰⁾ The increase in atomic LS -coupling on Pt ions as well as the deformation of crystal structure¹²⁾ significantly increases the antisymmetric spin-orbit coupling of $\text{Li}_2\text{Pt}_3\text{B}$. According to the first-principles band structure calculation, this enhancement of antisymmetric spin-orbit coupling is accompanied by the topological transition of the Fermi surfaces (FS topological transition).²¹⁾ The Fermi surfaces of $\text{Li}_2\text{Pd}_3\text{B}$ consist of several pairs of spin-split Fermi surfaces. On the other hand, the counterpart of some pairs vanishes in $\text{Li}_2\text{Pt}_3\text{B}$. According to recent studies of the crystal structure of solid solution $\text{Li}_2(\text{Pd}_{1-x}\text{Pt}_x)_3\text{B}$, the structural deformation occurs at approximately $x \sim 0.8$,¹²⁾ which is probably accompanied by the FS topological transition.

The purpose of this study is to clarify the effect of FS topological transition due to the antisymmetric spin-orbit coupling on the superconducting state. We here study the roles of three types of FS topological transition on the spin susceptibility in the superconducting state. In type (A), one of the spin-split Fermi surfaces vanishes owing to the substantial increase in the spin-orbit coupling [see Fig. 1(a)]. In type (B), the Fermi surface crosses the Dirac point with increasing spin-orbit coupling, as shown in Fig. 1(b). Finally, in type (C), one of the spin-split Fermi surfaces crosses a van-Hove singularity, as shown in Fig. 1(c). Our analysis is based on a single-band model, which cannot reproduce the electronic structure of $\text{Li}_2(\text{Pd}_{1-x}\text{Pt}_x)_3\text{B}$. However, some effects of FS topological transition are independent of the band structure, as shown below. We expect that the following results would be a key to resolve unsettled issues of $\text{Li}_2(\text{Pd}_{1-x}\text{Pt}_x)_3\text{B}$. Our results are

*E-mail address: marudai@phys.sc.niigata-u.ac.jp

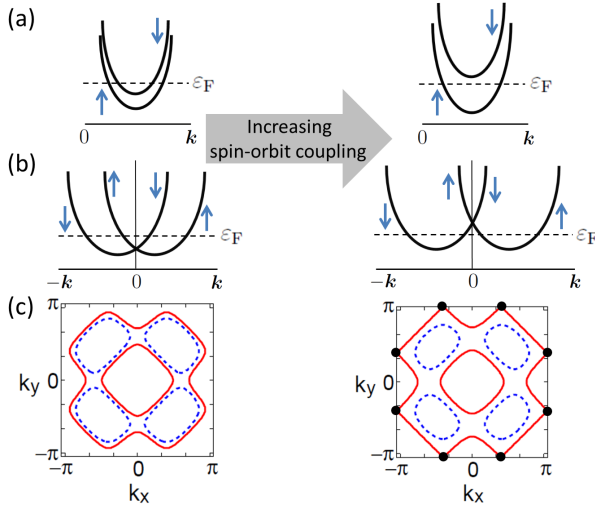


Fig. 1. (Color online) Schematic figure of FS topological transitions. (a) Type (A): One of the split Fermi surfaces vanishes around the top or bottom of the band. (b) Type (B): The Fermi level crosses the Dirac point. In figures (a) and (b), the thick solid lines show the two spin-split bands and the arrows show the spin of each band. (c) Type (C): A Fermi surface crosses the van-Hove singularities (closed circles). The dotted and solid lines show the Fermi surfaces of the ε_+ band and the ε_- band, respectively.

also applicable to other non-centrosymmetric superconductors with a large spin-orbit coupling. We introduce the model Hamiltonian in Sect. 2 and show the numerical results of spin susceptibility in Sect. 3. Some remarks are given in Sect. 4.

2. Model

We adopt the following single-band Hamiltonian;

$$H = \sum_{\mathbf{k},s} \varepsilon(\mathbf{k}) c_{\mathbf{k}s}^\dagger c_{\mathbf{k}s} + \alpha \sum_{\mathbf{k},s,s'} \mathbf{g}(\mathbf{k}) \cdot \boldsymbol{\sigma}_{ss'} c_{\mathbf{k}s}^\dagger c_{\mathbf{k}s'} + \frac{1}{2} \sum_{\mathbf{k},s,s'} [\Delta_{ss'}(\mathbf{k}) c_{\mathbf{k}s}^\dagger c_{-\mathbf{k}s'}^\dagger + \text{h.c.}], \quad (1)$$

where $c_{\mathbf{k}s}$ ($c_{\mathbf{k}s}^\dagger$) is the annihilation (creation) operator for an electron with a momentum \mathbf{k} and a spin s . The dispersion relation $\varepsilon(\mathbf{k})$ is assumed so that the FS topological transition occurs with increasing antisymmetric spin-orbit coupling. The chemical potential μ is involved in the dispersion relation and determined so that the electron density per site is n . The second term describes the antisymmetric spin-orbit coupling, which preserves the time reversal symmetry for the antisymmetric \mathbf{g} -vector $\mathbf{g}(-\mathbf{k}) = -\mathbf{g}(\mathbf{k})$. The spin-orbit coupling lifts the two-fold degeneracy in the band as $\varepsilon_{\pm}(\mathbf{k}) = \varepsilon(\mathbf{k}) \pm \alpha|\mathbf{g}(\mathbf{k})|$. In this research, we study the two-dimensional Rashba spin-orbit coupling with $\mathbf{g}(\mathbf{k}) = (-\sin k_y, \sin k_x, 0)$ as well as the three-dimensional cubic spin-orbit coupling with $\mathbf{g}(\mathbf{k}) = (\sin k_x, \sin k_y, \sin k_z)$.

We take into account the mean field of superconducting order parameters in the last term of Eq. (1). The order parameters $\Delta_{ss'}(\mathbf{k})$ involve both spin singlet and triplet components due to the spin-orbit coupling. We here ignore the spin triplet component and assume the s-wave spin singlet order parameter $[\Delta_{\uparrow\downarrow}(\mathbf{k}) = -\Delta_{\downarrow\uparrow}(\mathbf{k}) = \psi]$, since the spin susceptibility at zero temperature is independent of the symmetry of order parameters for a large spin-orbit coupling $|\Delta_{ss'}(\mathbf{k})| \ll \alpha$.^{13–15)}

Although the p -wave superconducting state of $\text{Li}_2\text{Pt}_3\text{B}$ has been indicated by several experimental results,^{6,12)} we do not touch this possibility since our analysis of the spin susceptibility cannot distinguish the p -wave superconducting state from the s -wave one. We take $|\psi| \leq 0.01$ so as to be small enough to satisfy the condition $|\Delta_{ss'}(\mathbf{k})| \ll \alpha$, as realized in most non-centrosymmetric superconductors.

3. Spin Susceptibility in the Superconducting State

In this section, we calculate the spin susceptibility in the superconducting state. We consider the zero temperature $T = 0$ throughout this paper. The spin susceptibility $\chi = \lim_{H \rightarrow 0} \langle M \rangle / H$ is obtained by calculating the magnetization $\langle M \rangle$ in the field \mathbf{H} and taking the limit $\mathbf{H} \rightarrow 0$. The Zeeman coupling term is introduced as $H_Z = -(g\mu_B/2) \sum_{\mathbf{k},s,s'} \mathbf{H} \cdot \boldsymbol{\sigma}_{ss'} c_{\mathbf{k}s}^\dagger c_{\mathbf{k}s'}$ where we assume $g = 2$ and μ_B is the Bohr magneton. We first study the two-dimensional systems with Rashba spin-orbit coupling. Later, we will show the results for three-dimensional systems with cubic spin-orbit coupling. For two-dimensional systems, we focus on the spin susceptibility in the ab -plane, since that along the c -axis is not reduced by the superconductivity.²²⁾ On the other hand, the spin susceptibility is isotropic in the cubic system. We discuss the spin susceptibility normalized by the normal state value χ_s/χ_n , where χ_s is the spin susceptibility in the superconducting state. The normal state value of spin susceptibility χ_n is calculated at $T = 0$ for $|\Delta_{ss'}(\mathbf{k})| = 0$.

3.1 Two-dimensional systems

First, we study two-dimensional systems with the Rashba spin-orbit coupling $\mathbf{g}(\mathbf{k}) = (-\sin k_y, \sin k_x, 0)$. The dispersion relation is assumed as

$$\varepsilon(\mathbf{k}) = 2t_1(\cos k_x + \cos k_y) + 4t_2 \cos k_x \cos k_y + 2t_3(\cos 2k_x + \cos 2k_y) - \mu. \quad (2)$$

The FS topological transition of type (A) occurs at $\alpha = 0.325$ for the parameters $(t_1, t_2, t_3, n) = (-0.25, 0.5, 0.8, 0.1)$, where the band width is $W = 8$. Figure 2(a) shows the normalized spin susceptibility χ_s/χ_n as a function of the spin-orbit coupling α . We see the discontinuous jump of the normalized spin susceptibility at $\alpha = 0.325$. This jump is caused by the sudden decrease in spin susceptibility in the normal state χ_n at the type (A) FS topological transition with increasing α . On the other hand, spin susceptibility in the superconducting state χ_s is not substantially affected by the FS topological transition, as shown in Fig. 2(a).

We clarify these changes by dividing the spin susceptibility into the Pauli part and Van-Vleck part. The Van-Vleck part of spin susceptibility is defined using the dynamical spin susceptibility in the normal state $\chi_n(\mathbf{q}, \omega)$ as $\chi_V = \lim_{\omega \rightarrow 0} \lim_{\mathbf{q} \rightarrow 0} \chi_n(\mathbf{q}, \omega)$. On the other hand, the spin susceptibility observed in experiments is obtained as $\chi_n = \lim_{\mathbf{q} \rightarrow 0} \lim_{\omega \rightarrow 0} \chi_n(\mathbf{q}, \omega)$. The Pauli part is the difference $\chi_P = \chi_n - \chi_V$. The Pauli part χ_P comes from the intraband contributions and is completely suppressed at $T = 0$. On the other hand, the Van-Vleck part χ_V comes from the interband transition between the ε_+ band and the ε_- band and is hardly affected by the superconductivity. Note that this Van-Vleck part χ_V is different from the usual T -independent Van-Vleck susceptibility arising from the orbital degrees of freedom. The

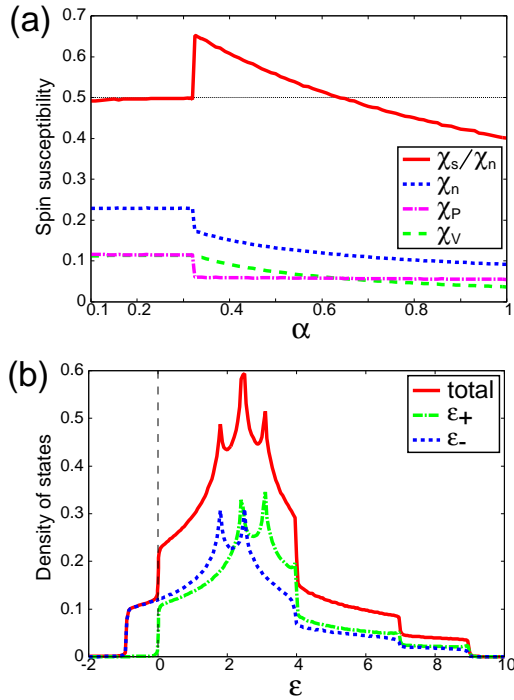


Fig. 2. (Color online) (a) Normalized spin susceptibility χ_s/χ_n in the two-dimensional systems with the Rashba spin-orbit coupling (solid line). We assume the dispersion relation Eq. (2) with $(t_1, t_2, t_3, n) = (-0.25, 0.5, 0.8, 0.1)$. The FS topological transition of type (A) occurs at $\alpha = 0.325$. The spin susceptibility in the normal state χ_n is shown by the dotted line. The Pauli part χ_P (dash-dotted line) and Van-Vleck part χ_V (dashed line) are shown for discussion. In Figs. 2(a), 3, and 4, the horizontal thin dotted line shows the normalized spin susceptibility $\chi_s/\chi_n = 1/2$ of conventional Rashba superconductors.²²⁾ (b) Density of states in the normal state at $\alpha = 0.325$. The solid line shows the total density of states. The density of states of the ϵ_+ band and that of the ϵ_- band are shown by the dash-dotted and dotted lines, respectively. The vertical dashed line shows the Fermi energy.

Van-Vleck part χ_V in our definition has a temperature dependence similarly to the Pauli part χ_P when the spin-orbit coupling α is much smaller than the Fermi energy. Thus, this χ_V is included in the spin part of the NMR Knight shift K_s , while the Van-Vleck susceptibility arising from the orbital degrees of freedom is included in the orbital part K_{orb} . When we focus on the spin susceptibility extracted from the spin part K_s , as often analyzed in the NMR experiment, the spin susceptibility is obtained as $\chi_n = \chi_P + \chi_V$ in the normal state, while it is almost equivalent to the Van-Vleck part $\chi_s \approx \chi_V$ in the superconducting state.

Because the Pauli part χ_P is proportional to the density of states at the Fermi level, the disappearance of the Fermi surface at the type (A) FS topological transition decreases χ_P as well as χ_n . This decrease occurs in a discontinuous manner in the two-dimensional systems since the density of states is discontinuous at the band edge [see Fig. 2(b)]. On the other hand, the spin susceptibility in the superconducting state is robust for the disappearance of the Fermi surface, since that comes from the Van-Vleck term χ_V . In this way, the normalized spin susceptibility χ_s/χ_n is increased at the type (A) FS topological transition with increasing the spin-orbit coupling. For a large spin-orbit coupling $\alpha > 0.325$, χ_s/χ_n gradually decreases with α , because of the decrease in the Van-Vleck

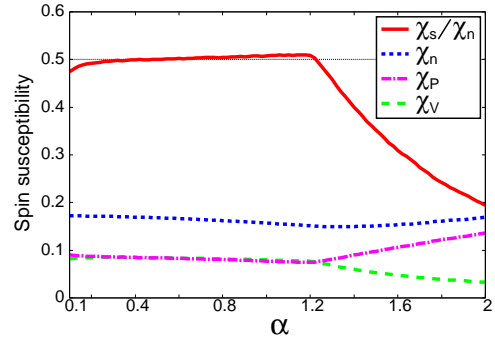


Fig. 3. (Color online) Normalized spin susceptibility χ_s/χ_n for $(t_1, t_2, t_3, n) = (-1, 0, 0, 0.1)$ in Eq. (2). The FS topological transition of type (B) occurs at $\alpha = 1.22$. The lines show the same quantities as in Fig. 2(a).

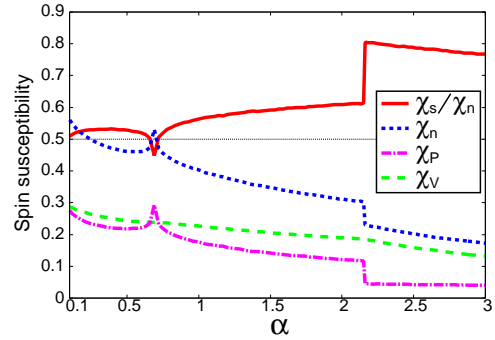


Fig. 4. (Color online) Normalized spin susceptibility χ_s/χ_n for $(t_1, t_2, t_3, n) = (-0.25, 0.5, 0.8, 0.8)$ in Eq. (2). The FS topological transition of type (C) occurs at $\alpha = 0.69$, and that of type (A) occurs at $\alpha = 2.16$. The lines show the same quantities as in Fig. 2(a).

term. It should be stressed that χ_s/χ_n is much larger than the canonical value $1/2$ when the spin-orbit coupling α is a little larger than the critical value $\alpha_c = 0.325$.

Next, we study the FS topological transition of type (B). For the parameters $(t_1, t_2, t_3, n) = (-1, 0, 0, 0.1)$ of Eq. (2), the Fermi surface crosses the Dirac point at $\alpha = 1.22$. Figure 3 shows the decrease in χ_s/χ_n for $\alpha > 1.22$ in sharp contrast to the FS topological transition of type (A). This is because the density of states at the Fermi energy increases and therefore the Pauli part χ_P increases with α for $\alpha > 1.22$.

The normalized spin susceptibility χ_s/χ_n is increased by the FS topological transition of type (C), as investigated by Fujimoto.¹³⁾ Our calculation reproduces his result, but the enhancement of normalized spin susceptibility is much smaller than that due to the type (A) FS topological transition. When we assume the parameters $(t_1, t_2, t_3, n) = (-0.25, 0.5, 0.8, 0.8)$ of Eq. (2), the FS topological transition of type (C) occurs at $\alpha = 0.69$. Figure 4 shows that χ_s/χ_n decreases at the transition $\alpha = 0.69$ and increases with increasing α for $\alpha > 0.69$. The increase in χ_s/χ_n for $\alpha > 0.69$ is less pronounced than that due to the type (A) transition. Indeed, we see a significant increase in χ_s/χ_n at $\alpha = 2.16$ where the FS topological transition of type (A) occurs.

3.2 Three-dimensional systems

We turn to three-dimensional systems with the cubic symmetry. The cubic spin-orbit coupling with $\mathbf{g}(\mathbf{k}) = (\sin k_x, \sin k_y, \sin k_z)$ is considered here. We assume the dispersion relation as,

$$\begin{aligned} \varepsilon(\mathbf{k}) = & 2t_1(\cos k_x + \cos k_y + \cos k_z) \\ & + 4t_2(\cos k_x \cos k_y + \cos k_y \cos k_z + \cos k_z \cos k_x) \\ & + 8t_3 \cos k_x \cos k_y \cos k_z \\ & + 2t_4(\cos 2k_x + \cos 2k_y + \cos 2k_z) - \mu. \end{aligned} \quad (3)$$

When we choose the parameters $(t_1, t_2, t_3, t_4, n) = (-0.8, 0.275, 0.1125, 0.8, 0.2)$, where the band width is $W = 17.24$, the Fermi surfaces show the topological transition of type (A) at $\alpha = 0.92$. Figure 5(a) shows the maximum χ_s/χ_n at this FS topological transition. On the other hand, the increase in χ_s/χ_n is not discontinuous in contrast to that in two-dimensional systems [see Fig. 2(a)]. This is because the density of states continuously decreases as $\rho(\varepsilon) \propto \sqrt{\varepsilon - \varepsilon_c}$ at the band edge $\varepsilon = \varepsilon_c$ [see Fig. 5(b)]. Because of the less singular properties in the density of states, the increase in the normalized spin susceptibility χ_s/χ_n due to the FS topological transition is less pronounced than that in two-dimensional systems.

A small enhancement of χ_s/χ_n in Fig. 5(a) from the conventional value $\chi_s/\chi_n = 2/3$ implies that there is another source of the large spin susceptibility χ_s/χ_n observed in $\text{Li}_2\text{Pt}_3\text{B}$.

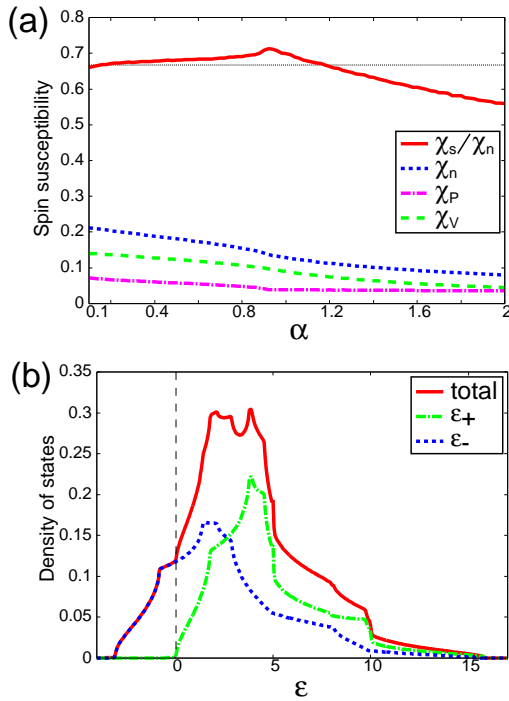


Fig. 5. (Color online) (a) Normalized spin susceptibility χ_s/χ_n in the three-dimensional systems with the cubic spin-orbit coupling. We assume the parameters $(t_1, t_2, t_3, t_4, n) = (-0.8, 0.275, 0.1125, 0.8, 0.2)$ in Eq. (3). The FS topological transition of type (A) occurs at $\alpha = 0.92$. The lines show the same quantities as in Fig. 2(a). In Figs. 5(a) and 6, the horizontal thin dotted line shows the normalized spin susceptibility $\chi_s/\chi_n = 2/3$ of conventional cubic non-centrosymmetric superconductors.^{13,14} (b) Density of states in the normal state at $\alpha = 0.92$. The vertical dashed line shows the Fermi energy. The lines show the same quantities as in Fig. 2(b).

We here show a case in which a large χ_s/χ_n close to unity is realized. When we assume the parameters $(t_1, t_2, t_3, t_4, n) = (-0.8, 0.275, 0.1125, 0.8, 0.9)$ in Eq. (3), the Fermi surface of the ε_- band and that of the ε_+ band cross the van-Hove singularity at $\alpha = 0.82$ and $\alpha = 2.3$, respectively. With further increase in the spin-orbit coupling, the Fermi surface of the ε_+ band vanishes at $\alpha = 3.6$. We obtain a large normalized spin susceptibility $\chi_s/\chi_n > 0.9$ for $\alpha > 3.6$, as shown in Fig. 6.

We explain such a large spin susceptibility in the superconducting state by discussing again the Pauli part and Van-Vleck part of spin susceptibility. For simplicity, we consider a small electron pocket Fermi surface of heavy ε_+ band and a small hole pocket of light ε_- band. The Pauli part of spin susceptibility is proportional to the density of states,

$$\rho(\epsilon_F) = \frac{\sqrt{2m_e^3(\epsilon_F - \epsilon_{c+})}}{4\pi^2} + \frac{\sqrt{2m_h^3(\epsilon_{c-} - \epsilon_F)}}{4\pi^2},$$

where the first term (second term) comes from the heavy electron band (light hole band). We denoted the band edge of each band, ϵ_{c+} and ϵ_{c-} , and assume the effective mass, $m_e \gg m_h$. When the electron pocket vanishes with increasing antisymmetric spin-orbit coupling, the density of states is significantly decreased as

$$\rho(\epsilon_F) = \frac{\sqrt{2m_h^3(\epsilon_{c-} - \epsilon_F)}}{4\pi^2}.$$

The decrease in the density of states leads to a decrease in the Pauli part spin susceptibility, while the Van-Vleck part is hardly affected. Thus, the normalized spin susceptibility $\chi_s/\chi_n = \chi_v/(\chi_P + \chi_v)$ shows a substantial increase as it approaches the FS topological transition of type (A), when the spin-split Fermi surfaces have different effective masses and the Fermi surface of heavy band vanishes, as in the case of our model adopted in Fig. 6. This is a possible mechanism of the large spin susceptibility χ_s/χ_n in $\text{Li}_2\text{Pt}_3\text{B}$, although the possibility of another source for realizing a small Pauli term is not excluded. We would like to stress that such a small Pauli term is not realized by a small antisymmetric spin-orbit coupling compared with the Fermi energy.

Indeed, successive FS topological transitions from $\text{Li}_2\text{Pd}_3\text{B}$ to $\text{Li}_2\text{Pt}_3\text{B}$ have been indicated by the first-principles band structure calculations.^{20,21} Thus, the intriguing topology of the Fermi surface in $\text{Li}_2(\text{Pd}_{1-x}\text{Pt}_x)_3\text{B}$ may be the source of the unusual magnetic properties in the superconducting state. A decrease in the density of states with increasing concentration of Pt ions has not been clearly observed,⁷ indicating that our proposal is not likely realized. However, the multiband structure of $\text{Li}_2(\text{Pd}_{1-x}\text{Pt}_x)_3\text{B}$ does not allow such a simple discussion. FS topological transitions of $\text{Li}_2(\text{Pd}_{1-x}\text{Pt}_x)_3\text{B}$ are partly due to the multiband structure, and the single-band model adopted in this paper does not precisely reproduce the electronic structure of $\text{Li}_2(\text{Pd}_{1-x}\text{Pt}_x)_3\text{B}$. The analysis of a realistic model is desired to elucidate the superconducting state of $\text{Li}_2(\text{Pd}_{1-x}\text{Pt}_x)_3\text{B}$.

4. Summary and Discussion

We have investigated the spin susceptibility of non-centrosymmetric superconductors, which is accompanied by the topological transition of Fermi surfaces owing to the antisymmetric spin-orbit coupling. When one of the Fermi sur-

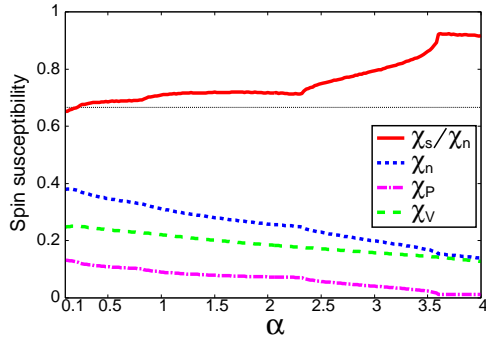


Fig. 6. (Color online) Normalized spin susceptibility χ_s/χ_n for $(t_1, t_2, t_3, t_4, n) = (-0.8, 0.275, 0.1125, 0.8, 0.9)$ in Eq. (3). The FS topological transition of type (C) occurs at $\alpha = 0.82$ and $\alpha = 2.3$, and that of type (A) occurs at $\alpha = 3.6$.

faces of the spin-split band vanishes [FS topological transition of type (A)], the normalized spin susceptibility χ_s/χ_n is increased. On the other hand, χ_s/χ_n is decreased by the FS topological transition of type (B) in which the Fermi level crosses the Dirac point. The spin susceptibility χ_s/χ_n increases when the Fermi surface crosses van-Hove singularities [FS topological transition of type (C)], but the increase is smaller than that due to type (A). We obtain the maximum χ_s/χ_n at the type (A) FS topological transition, and a large χ_s/χ_n for the antisymmetric spin-orbit coupling α larger than the critical value.

These behaviors of the spin susceptibility are understood in terms of the density of states. The density of states depends on the band structure; however, it shows a universal change at the FS topological transition. Thus, our results on the changes at the FS topological transition are qualitatively independent of the band structure. Note that these results are also independent of the symmetry of superconductivity.

The effects of FS topological transitions are pronounced in the two-dimensional systems because of the discontinuous jump of the density of states at the band edge. Even in three-dimensional systems, the spin susceptibility is almost unchanged through the superconducting transition, when successive transitions of types (A) and (C) occur. We obtained a large normalized spin susceptibility $\chi_s/\chi_n > 0.9$, which is consistent with the NMR Knight shift measurement for $\text{Li}_2\text{Pt}_3\text{B}$ ^{6,12)} within the experimental resolution. Generally, such a large normalized spin susceptibility is obtained when the density of states is significantly decreased by the antisymmetric spin-orbit coupling. We showed an example of such a band structure. Although our single-band model does not reproduce the multiband structure of $\text{Li}_2\text{Pt}_3\text{B}$, our finding indi-

cates the important roles of FS topological transitions. Indeed, the band structure calculation shows a lot of topological transitions in $\text{Li}_2\text{Pt}_3\text{B}$ owing to the large spin-orbit coupling, but not in $\text{Li}_2\text{Pd}_3\text{B}$ because of the small spin-orbit coupling.^{20,21)} In order to elucidate the effect of the intriguing topology of the Fermi surface on the superconducting phase in $\text{Li}_2\text{Pt}_3\text{B}$, it is desired to study the multiorbital model, which precisely describes the electronic structure of $\text{Li}_2(\text{Pd}_{1-x}\text{Pt}_x)_3\text{B}$.

Acknowledgements

The authors are grateful to T. Shishidou and G.-q. Zheng for fruitful discussions. This work was supported by a Grant-in-Aid for Scientific Research on Innovative Areas “Heavy Electrons” (No. 23102709) from MEXT, and by a Grant-in-Aid for Young Scientists (B) (No. 24740230) from JSPS.

- 1) *Non-centrosymmetric Superconductors Introduction and Overview*, ed. E. Bauer and M. Sigrist (Springer, Heidelberg, 2012) Lecture Notes in Physics, Vol. 847.
- 2) K. Togano, P. Badica, Y. Nakamori, S. Orimo, H. Takeya, and K. Hirata: Phys. Rev. Lett. **93** (2004) 247004.
- 3) P. Badica, T. Kondo, and K. Togano: J. Phys. Soc. Jpn. **74** (2005) 1014.
- 4) R. Khasanov, I. L. Landau, C. Baines, F. La Mattina, A. Maisuradze, K. Togano, and H. Keller: Phys. Rev. B **73** (2006) 214528.
- 5) H. Q. Yuan, D. F. Agterberg, N. Hayashi, P. Badica, D. Vandervelde, K. Togano, M. Sigrist, and M. B. Salamon: Phys. Rev. Lett. **97** (2006) 017006.
- 6) M. Nishiyama, Y. Inada, and G.-q. Zheng: Phys. Rev. Lett. **98** (2007) 047002.
- 7) H. Takeya, M. ElMassalami, S. Kasahara, and K. Hirata: Phys. Rev. B **76** (2007) 104506.
- 8) T. Yokoya, T. Muro, I. Hase, H. Takeya, K. Hirata, and K. Togano: Phys. Rev. B **71** (2005) 092507.
- 9) M. Nishiyama, Y. Inada, and G.-q. Zheng: Phys. Rev. B **71** (2005) 220505(R).
- 10) H. Takeya, K. Hirata, K. Yamaura, K. Togano, M. El Massalami, R. Rapp, F. A. Chaves, and B. Ouladdiaf: Phys. Rev. B **72** (2005) 104506.
- 11) D. C. Peets, G. Eguchi, M. Kriener, S. Harada, Sk. Md. Shamsuzzamen, Y. Inada, G.-Q. Zheng, and Y. Maeno: Phys. Rev. B **84** (2011) 054521.
- 12) S. Harada, J. J. Zhou, Y. G. Yao, Y. Inada, and G.-q. Zheng: Phys. Rev. B **86** (2012) 220502(R).
- 13) S. Fujimoto: J. Phys. Soc. Jpn. **76** (2007) 034712.
- 14) K. V. Samokhin: Phys. Rev. B **76** (2007) 094516.
- 15) Y. Yanase and M. Sigrist: J. Phys. Soc. Jpn. **76** (2007) 124709.
- 16) S. P. Mukherjee and T. Takimoto: Phys. Rev. B **86** (2012) 134526.
- 17) H. Shimahara: J. Phys. Soc. Jpn. **82** (2013) 024703.
- 18) Y. Yanase and M. Sigrist: J. Phys. Soc. Jpn. **76** (2007) 043712.
- 19) Y. Yanase and M. Sigrist: J. Phys. Soc. Jpn. **77** (2008) 124711.
- 20) K.-W. Lee and W. E. Pickett: Phys. Rev. B **72** (2005) 174505.
- 21) T. Shishidou and T. Oguchi: preprint (2012).
- 22) P. A. Frigeri, D. F. Agterberg, and M. Sigrist: New J. Phys. **6** (2004) 115.